A Genome-Wide Screen for Genes Affecting Spontaneous Direct-Repeat Recombination in *Saccharomyces cerevisiae*

Daniele Novarina,* Ridhdhi Desai,† Jessica A. Vaisica,† Jiongwen Ou,† Mohammed Bellaoui,†,1 Grant W. Brown,†,2 and Michael Chang*,3

*European Research Institute for the Biology of Ageing, University of Groningen, University Medical Center Groningen, 9713 AV Groningen, the Netherlands and †Department of Biochemistry and Donnelly Centre, University of Toronto, Toronto, ON M5S 3E1, Canada

ORCID IDs: 0000-0001-5213-9344 (J.A.V.); 0000-0002-9002-5003 (G.W.B.); 0000-0002-1706-3337 (M.C.)

ABSTRACT Homologous recombination is an important mechanism for genome integrity maintenance, and several homologous recombination genes are mutated in various cancers and cancer-prone syndromes. However, since in some cases homologous recombination can lead to mutagenic outcomes, this pathway must be tightly regulated, and mitotic hyper-recombination is a hallmark of genomic instability. We performed two screens in *Saccharomyces cerevisiae* for genes that, when deleted, cause hyper-recombination between direct repeats. One was performed with the classical patch and replica-plating method. The other was performed with a high-throughput replica-pinning technique that was designed to detect low-frequency events. This approach allowed us to validate the high-throughput replica-pinning methodology independently of the replicative aging context in which it was developed. Furthermore, by combining the two approaches, we were able to identify and validate 35 genes whose deletion causes elevated spontaneous direct-repeat recombination. Among these are mismatch repair genes, the Sgs1-Top3-Rmi1 complex, the RNase H2 complex, genes involved in the oxidative stress response, and a number of other DNA replication, repair and recombination genes. Since several of our hits are evolutionarily conserved, and repeated elements constitute a significant fraction of mammalian genomes, our work might be relevant for understanding genome integrity maintenance in humans.

Homologous recombination (HR) is an evolutionarily conserved pathway that can repair DNA lesions, including double-strand DNA breaks (DSBs), single-strand DNA (ssDNA) gaps, collapsed replication forks, and interstrand crosslinks, by using a homologous sequence as the repair template . HR is essential for the maintenance of genome integrity, and several HR genes are mutated in human diseases, especially cancers and cancer-prone syndromes (Krejci *et al.*, 2012; Symington *et al.*, 2014). HR is also required for meiosis (Hunter 2015) and is important for proper telomere function (Claussin and Chang 2015). The yeast *Saccharomyces cerevisiae* has been a key model organism for determining the mechanisms of eukaryotic recombination. Our current understanding of the HR molecular pathway comes mainly from the study of DSB repair. However, most mitotic HR events are likely not due to the repair of DSBs (Claussin *et al.*, 2017), and can be triggered by diverse DNA structures and lesions, including DNA nicks, ssDNA gaps, arrested or collapsed replication forks, RNA-DNA hybrids and noncanonical secondary structures (Symington *et al.*, 2014). An essential intermediate in recombination is ssDNA, which, in the case of a DSB, is generated by resection of the DSB ends by nucleases. Rad52 stimulates the loading of Rad51 onto ssDNA, which in turn mediates

homologous pairing and strand invasion, with the help of Rad54, Rad55, and Rad57. After copying the homologous template, recombination intermediates are resolved with the help of nucleases and helicases, and the HR machinery is disassembled (Symington *et al.*, 2014).

While HR is important for genome integrity, excessive or unregulated recombination in mitotic cells can be deleterious. Indeed, even though HR is generally considered an error-free DNA repair pathway, outcomes of HR can be mutagenic. For instance, recombination between ectopic homolog sequences can lead to gross chromosomal rearrangements (Heyer 2015). Mutations and chromosomal aberrations can be the outcome of recombination between slightly divergent DNA sequences, a process termed "homeologous recombination" (Spies and Fishel 2015). Allelic recombination between homologous chromosomes can lead to loss of heterozygosity (LOH) (Aguilera and García-Muse 2013). Finally, the copying of the homologous template occurs at lower fidelity than is typical for replicative DNA polymerases, resulting in mutagenesis (McVey *et al.*, 2016). For these reasons, the HR process must be tightly controlled, and spontaneous hyper-recombination in mitotic cells is a hallmark of genomic instability (Aguilera and García-Muse 2013; Heyer 2015).

Pioneering mutagenesis-based screens led to the identification of hyper-recombination mutants (Aguilera and Klein 1988; Keil and McWilliams 1993). Subsequently, several systematic screens were performed with the yeast knockout (YKO) collection to identify genes whose deletion results in a spontaneous hyper-recombinant phenotype. In particular, Alvaro *et al.* screened an indirect phenotype, namely elevated spontaneous Rad52 focus formation in diploid cells, which led to the identification of hyper-recombinant as well as recombination-defective mutants (Alvaro *et al.*, 2007). A second screen for elevated Rad52 foci in haploid cells identified additional candidate recombination genes (Styles *et al.*, 2016), although the recombination rates of these were not assessed directly. A distinct screen of the YKO collection measured elevated spontaneous LOH events in diploid cells, which arise through recombination between homologous chromosomes or as a consequence of chromosome loss (Andersen *et al.*, 2008).

Here we describe two systematic genome-scale screens measuring spontaneous recombination in haploid cells, since the sister chromatid is generally a preferred template for mitotic recombination relative to the homologous chromosome, both in yeast and mammalian cells (Johnson and Jasin 2000; Kadyk and Hartwell 1992). We use a direct-repeat recombination assay (Smith and Rothstein 1999), because recombination between direct repeats can have a significant impact on the stability of mammalian genomes, where tandem and interspersed repeated elements, such as LINEs and SINEs, are very abundant (George and Alani 2012; López-Flores and Garrido-Ramos 2012).

Recombination rate screens were performed both with the classical patch and replica-plating method and with our recently developed high-throughput replica-pinning technique, which was designed for high-throughput screens involving low-frequency events (Novarina *et al.*, 2020). High-throughput replica-pinning is based on the concept that, by robotically pinning an array of yeast strains many times in parallel, several independent colonies per strain can be analyzed at the same time, giving a semi-quantitative estimate of the rate at which a specific low-frequency event occurs in each strain. We used both approaches to screen the YKO collection with the direct-repeat recombination assay. Bioinformatic analysis and direct comparison of the two screens confirmed the effectiveness of the high-throughput replica-pinning methodology. Together, we identified and validated 35 genes whose deletion results in elevated spontaneous direct-repeat recombination, many of which have homologs or functional counterparts in humans.

MATERIALS AND METHODS

Yeast strains and growth conditions
Standard yeast media and growth conditions were used (Sherman 2002; Treco and Lundblad 2001). All yeast strains used in this study are derivatives of the BY4741 genetic background (Brachmann *et al.*, 1998) and are listed in Supporting Information, Table S1.

Patch and replica-plating screen
To create a recombination assay strain compatible with Synthetic Genetic Array (SGA) methodology (Kuzmin *et al.*, 2016), the *leu2ΔEcoRI-URA3-leu2ΔBstEII* direct repeat recombination reporter (Smith and Rothstein 1999) was introduced into Y5518 by PCR of the *LEU2* locus from W1479-11C, followed by transformation of Y5518 and selection on SD-ura. Correct integration was confirmed by PCR, and the resulting strain was designated JOY90. JOY90 was then crossed to the *MAT***a** yeast knockout (YKO) collection ((Giaever *et al.*, 2002); gift of C. Boone, University of Toronto), using SGA methodology (Kuzmin *et al.*, 2016). Following selection on SD-his-arginine-lysine-uracil+G418+ClonNat+canavanine+thialysine, the resulting strains have the genotype *MAT***a** *xxxΔ::kanMX mfa1Δ::MFA1pr-HIS3 leu2ΔEcoRI::URA3-HOcs::leu2ΔBstEII his3Δ1 ura3Δ0 met15Δ0 lyp1Δ can1Δ::natMX*, where *xxxΔ::kanMX* indicates the YKO gene deletion in each resulting strain.

Each YKO strain carrying the recombination reporter was streaked for single colonies on SD-ura. Single colonies were then streaked in a 1 cm × 1 cm patch on YPD, incubated at 30° for 24 h, and then replica-plated to SD-leu to detect recombination events as papillae on the patch. RDY9 (wild-type) and RDY13 (*elg1Δ::kanMX*; positive control (Bellaoui *et al.*, 2003; Ben-Aroya *et al.*, 2003)) were included on each plate. The papillae on SD-leu were scored by visual inspection relative to the control strains, yielding 195 positives (Table S2). The 195 positives were tested in a fluctuation test of 5 independent cultures, and those with a recombination rate of at least 2×10^{-5} (approximately twofold greater than that of RDY9) were identified (43 strains; Table S2). Positives from the first fluctuation tests (except *slm3Δ* and *pex13Δ*, where rates could not be determined due to the large numbers of 'jackpot' cultures where all colonies had a recombination event) were assayed further, again with 5 cultures per fluctuation test. Thirty-three gene deletion mutants displayed a statistically supported increase in recombination rate (Table S2, Figure 1D), using a one-sided Student's *t*-test with a cutoff of $P = 0.05$.

Fluctuation tests of spontaneous recombination rates
Fluctuation tests as designed by Luria and Delbrück (Luria and Delbrück 1943) were performed by transferring entire single colonies from YPD plates to 4 ml of YPD liquid medium. Cultures were grown at 30° to saturation. 100 μl of a 10^5-fold dilution were plated on a fully supplemented SD plate and 200 μl of a 10^2-fold dilution were plated on an SD-leu plate. Colonies were counted after incubation at 30° for 3 days. The number of recombinant (leu+) colonies per 10^7 viable cells was calculated, and the median value was used to determine the recombination rate by the method of the median (Lea and Coulson 1949).

High-throughput replica pinning screen
High-throughput manipulation of high-density yeast arrays was performed with the RoToR-HDA pinning robot (Singer Instruments).
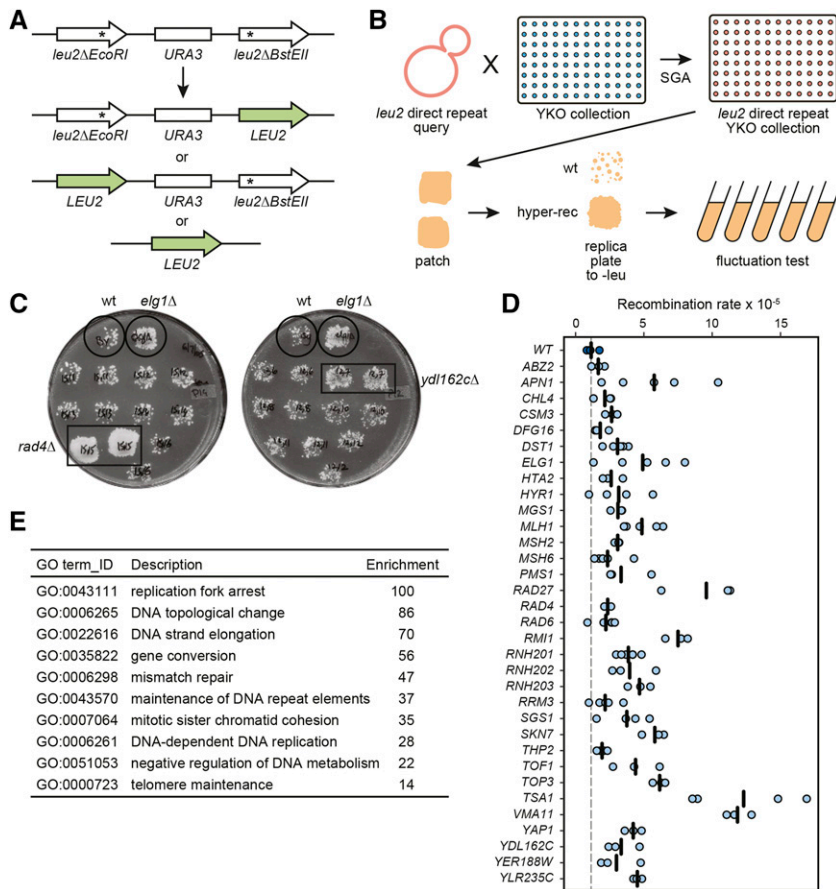
Figure 1 A genome-wide patching and replica plating screen for mutants with increased direct-repeat recombination. (A) The *leu2* direct-repeat recombination assay. Spontaneous recombination between two *leu2* heteroalleles, either through gene conversion or intra-chromosomal single strand annealing (SSA), yields a functional *LEU2* gene. (B) Schematic representation of the screen based on patching and replica plating. The *leu2* direct-repeat recombination cassette was introduced into the yeast deletion collection (YKO) by crossing the collection with a query strain containing the cassette. Haploid strains containing each gene deletion and the recombination cassette were isolated using SGA methodology. Each strain was patched on rich medium and replica-plated to selective medium, where hyper-recombinant mutants form papillae on the surface of the patch. Recombination rates were measured for positives from the patch assay using fluctuation tests. (C) Example plates from the patch assay. Each plate bears a negative control (wild type) and a positive control (*elg1Δ*). Two positive hits from the screen (*rad4Δ*, *ydl162cΔ*) are shown. (D) Recombination rates are plotted for the validated positives from the patch screen, alongside the wild-type strain. Each data point is from an independent fluctuation test, with n ≥ 3 for each strain. The vertical bars indicate the mean recombination rate for each strain. (E) The top 10 statistically supported GO terms enriched in the hits from the patch assay screen are shown, with the -fold enrichment for each term.

The *MAT***a** yeast deletion collection (EUROSCARF) was arrayed in 1536 format (each strain in quadruplicate). The *leu2ΔEcoRI-URA3-leu2ΔBstEII* marker to measure direct-repeat recombination (Smith and Rothstein 1999) was introduced into the deletion collection through synthetic genetic array (SGA) methodology (Kuzmin *et al.*, 2016) using the JOY90 query strain. The procedure was performed twice in parallel to generate two sets of the yeast deletion collection containing the *leu2* direct-repeat recombination reporter. Each plate of each set was then pinned onto six YPD+G418 plates (48 replicates per strain in total), incubated for one day at 30° and then scanned with a flatbed scanner. Subsequently, each plate was pinned onto SD-leu solid medium and incubated for two days at 30° to select recombination events. Finally, all plates were re-pinned on SD-leu solid medium and incubated for one day at 30° before scanning. Colony area measurement was performed using the ImageJ software package (Schneider *et al.*, 2012) and the ScreenMill Colony Measurement Engine plugin (Dittmar *et al.*, 2010), to assess colony circularity and size in pixels. Colony data were filtered to exclude artifacts by requiring a colony circularity score greater than 0.8. Colonies with a pixel area greater than 50% of the mean pixel area were scored for strains pinned to YPD+G418. Following replica-pinning to SD-leu, colonies were scored if the pixel area was greater than 10% of the mean pixel area for the same strain on YPD+G418. For each deletion strain, the ratio of recombinants (colonies on SD-leu) to total colonies (colonies on YPD+G418) is the recombinant frequency (Table S3). Strains where fewer than 10 colonies grew on YPD+G418 were removed from consideration, as were the 73 YKO collection strains

carrying an additional *msh3* mutation (Lehner *et al.*, 2007). The final filtered data are presented in Table S4.

Gene Ontology enrichment analysis and functional annotation

GO term analysis was performed using the GO term finder tool (http://go.princeton.edu/) using a P-value cutoff of 0.01 and applying Bonferroni correction, querying biological process enrichment for each gene set. GO term enrichment results were further processed with REVIGO (Supek *et al.*, 2011) using the "Medium (0.7)" term similarity filter and simRel score as the semantic similarity measure. Terms with a frequency greater than 15% in the REViGO output were eliminated as too general. Gene lists used for the GO enrichment analyses are in Table 1, and the lists of enriched GO terms obtained are provided in Table S6. Human orthologs in Table 3 were identified using YeastMine (https://yeastmine.yeastgenome.org/yeastmine; accessed June 25, 2019). Protein-protein interactions were identified using GeneMania (https://genemania.org/; (Warde-Farley *et al.*, 2010)), inputting the 35 validated hyper-rec genes, and selecting only physical interactions, zero resultant genes, and equal weighting by network. Network edges were reduced to a single width and nodes were annotated manually using gene ontology from the *Saccharomyces* Genome Database (https://www.yeastgenome.org). Network annotations were made with the Python implementation of Spatial Analysis of Functional Enrichment (SAFE) ((Baryshnikova 2016); https://github.com/baryshnikova-lab/safepy). The yeast genetic interaction similarity network and its functional domain annotations were obtained from (Costanzo *et al.*, 2016). The genetic

Table 1 Hyper-recombination genes from the patch assay and pinning assay screens

Patch Assay			Pinning Assay Hyper-Rec			
Gene name	Mean recombination rate[a]	Standard deviation	p-value[b]	Gene name	Recombinant colonies (%)	Gene name	Recombinant colonies (%)
WT	1.14E-05	2.84E-06		CSM1	100	RNH201	90
TSA1	1.23E-04	3.64E-05	7.76E-05	ELG1	100	YGL159W	90
VMA11	1.19E-04	7.62E-06	1.27E-08	MSH2	100	YJL043W	90
RAD27	9.39E-05	2.59E-05	1.26E-04	RAD27	100	YLR279W	90
RMI1	7.50E-05	6.85E-06	2.65E-07	RRM3	100	YOR082C	90
TOP3	6.15E-05	3.80E-06	1.13E-07	SGS1	100	ARP8	88
SKN7	5.80E-05	6.85E-06	2.20E-06	TSA1	100	BIO3	88
APN1	5.75E-05	2.97E-05	3.79E-03	DST1	98	COX7	88
ELG1	5.09E-05	1.30E-05	1.73E-04	RNH202	98	DCS2	88
MLH1	4.86E-05	1.15E-05	3.43E-05	RNH203	98	DDC1	88
RNH203	4.68E-05	6.79E-06	1.31E-05	MLH1	96	FUS2	88
YLR235C	4.52E-05	2.57E-06	6.11E-07	NUP170	96	HST3	88
TOF1	4.39E-05	1.40E-05	9.45E-04	PMS1	96	KIP1	88
YAP1	4.22E-05	5.04E-06	8.67E-06	ALE1	94	MFT1	88
RNH202	3.96E-05	1.38E-05	1.96E-03	APN1	94	MNT2	88
RNH201	3.86E-05	6.08E-06	1.91E-06	NFI1	94	MRPL51	88
SGS1	3.75E-05	1.42E-05	2.25E-03	YGR117C	94	NIT3	88
YDL162C	3.34E-05	9.73E-06	1.38E-03	YML020W	94	PCL10	88
PMS1	3.33E-05	1.28E-05	3.46E-03	YMR166C	94	PET123	88
HYR1	3.16E-05	1.74E-05	1.85E-02	YOR072W	94	PHM8	88
MGS1	3.10E-05	3.83E-06	6.14E-05	RPL23A	94	REC114	88
MSH2	3.09E-05	1.34E-06	1.55E-06	DIA2	92	RGS2	88
DST1	3.07E-05	6.56E-06	1.15E-04	EFT1	92	SCO1	88
YER188W	2.99E-05	1.27E-05	9.90E-03	MDM1	92	SPR1	88
CSM3	2.64E-05	3.65E-06	2.78E-04	MSN4	92	TOM5	88
HTA2	2.60E-05	6.24E-06	1.87E-03	PNS1	92	ULS1	88
RAD4	2.35E-05	2.46E-06	1.73E-03	RMI1	92	YDL009C	88
MSH6	2.34E-05	1.02E-05	1.68E-02	RRT14	92	YEL020C	88
RAD6	2.22E-05	7.25E-06	7.23E-03	SAC3	92	YGL042C	88
RRM3	2.16E-05	8.30E-06	1.54E-02	YDR230W	92	YJL017W	88
CHL4	2.14E-05	5.86E-06	9.36E-03	YLR235C	92	YJR018W	88
THP2	1.94E-05	2.95E-06	2.52E-03	YNL122C	92	YJR124C	88
DFG16	1.80E-05	4.48E-06	2.44E-02	YTA7	92	YKL091C	88
ABZ2	1.66E-05	3.93E-06	4.25E-02	FSH1	90	YKL162C	88
				GET3	90	YNL179C	88
				KGD2	90	YOR309C	88
				MID2	90	YOR333C	88
				POL32	90		

[a] Recombination rate from Table S2.
[b] p-values from one-sided Student's t-test.

interaction scores for *YER188W*, *DFG16*, *VMA11*, and *ABZ2* were downloaded from the Cell Map (http://thecellmap.org/; accessed January 9, 2020),

Statistical analysis

Statistical analysis was performed in Excel or R (https://cran.r-project.org/).

Data availability

Strains are available upon request. Table S1 lists all the strains used in this study. Table S2 contains the fluctuation test data from the patch screen. Table S3 contains the raw high-throughput replica pinning screen data. Table S4 contains the filtered pinning screen data. Table S5 contains the fluctuation test data from the pinning screen. Table S6 contains the GO term enrichment data. Supplemental material available at figshare: https://doi.org/10.25387/g3.11830833.

RESULTS

A genetic screen for elevated spontaneous direct-repeat recombination

The *leu2* direct-repeat recombination assay (Smith and Rothstein 1999) can detect both intra-chromosomal and sister chromatid recombination events (Figure 1A). Two nonfunctional *leu2* het-eroalleles are separated by a 5.3 kb region containing the *URA3* marker. Reconstitution of a functional *LEU2* allele can occur either via gene conversion (either inter- or intra-chromatid), which maintains the *URA3* marker, or via intra-chromosomal single strand annealing (SSA), where the *URA3* marker and one of the *leu2* repeats are lost (Symington *et al.*, 2014). Both recombination events can be selected on media lacking leucine. We used this assay to systematically screen the yeast knockout (YKO) collection for genes whose deletion results in hyper-recombination between direct repeats (Figure 1B). We introduced the *leu2* direct-repeat recombination reporter into the YKO collection via synthetic

genetic array (SGA) technology (Kuzmin *et al.*, 2016). Each of the ~4500 obtained strains was then patched on non-selective plates and replica-plated to plates lacking leucine to detect spontaneous recombination events as papillae on the replica-plated patches (Figure 1C). We included a wild-type control and a hyper-recombinant *elg1Δ* control (Bellaoui *et al.*, 2003; Ben-Aroya *et al.*, 2003) on every plate for reference. The recombination rates for 195 putative hyper-rec mutants identified by replica-plating (Table S2) were measured by a fluctuation test. Strains with a recombination rate greater than $2x10^{-5}$ (approximately twofold of the wild-type rate; 38 strains) were assayed in triplicate (or more). Thirty-three gene deletion mutant strains with a statistically supported increase in direct-repeat recombination rate relative to the wild-type control were identified (Figure 1D, Table S2, Table 1). The genes identified showed a high degree of enrichment for GO terms reflecting roles in DNA replication and repair (Figure 1E).

A high-throughput screen for altered spontaneous direct-repeat recombination

We recently developed a high-throughput replica-pinning method to detect low-frequency events, and validated the scheme in a genome-scale mutation frequency screen (Novarina *et al.*, 2020). To complement the data obtained with the classical screening approach, and to test our new methodology independently of the replicative aging context in which it was developed, we applied it to detect changes in spontaneous direct-repeat recombination (Figure 2A). We again introduced the *leu2* direct-repeat recombination reporter into the YKO collection. The collection was then amplified by parallel high-throughput replica-pinning to yield 48 colonies per gene deletion strain. After one day of growth, all colonies were replica-pinned (twice, in series) to media lacking leucine to select for recombination events. Recombinant frequencies (a proxy for the spontaneous recombination rate) were calculated for each strain of the collection (Figure 2B, Table S3, Table S4). As a reference, recombinant frequencies for the wild type (46%) and for a recombination-deficient *rad54Δ* strain (21%) obtained in a pilot replica-pinning experiment of 3000 colonies are indicated. In the screen itself, where 48 colonies were assessed, the wild type (*his3Δ::kanMX*) had a recombinant frequency of 56%. Notably, a group of strains from the YKO collection carry an additional mutation in the mismatch repair gene *MSH3* (Lehner *et al.*, 2007). Given the elevated spontaneous recombination rates of several mismatch repair-deficient strains (Figure 1D), we suspected that these *msh3* strains would display increased recombinant frequencies, independently of the identity of the intended gene deletion. Indeed, the distribution of recombinant frequencies for *msh3* strains (median: 74%) is shifted toward higher values compared to the overall distribution of the YKO collection (median: 60%) (Figure 2B). The 73 *msh3* strains were excluded from further analysis.

To explore the overall quality of the high-throughput replica-pinning screen and to determine a cutoff in an unbiased manner, we performed Cutoff Linked to Interaction Knowledge (CLIK) analysis (Dittmar *et al.*, 2013). The CLIK algorithm identified an enrichment of highly interacting genes at the top and at the bottom of our gene list (ranked according to recombinant frequency), confirming the overall high quality of our screen, and indicating that we were able to detect both hyper- and hypo-recombinogenic mutants (Figure 2C). The cutoff indicated by CLIK corresponds to a recombinant frequency of 87% for the hyper-recombination strains (75 genes; Table 1), and of 33% for the recombination-deficient strains (122 genes; Table 2).

Hyper-recombination genes: We assessed the functions of the 75 hyper-recombination genes identified by our high-throughput screen (Figure 2D). As with the genes identified in the patch screen, the genes identified in the pinning screen were enriched for DNA replication and repair functions. Most importantly, at the very top of our hyper-recombination gene list (with 96–100% recombinant frequency), 11 out of 13 genes were identified in the patch screen and validated by fluctuation analysis (Table S2). We tested the two additional genes, *CSM1* and *NUP170*, by fluctuation analysis, and found that both had a statistically supported increase in recombination rate (Figure 2E and Table S5). Eighteen validated hyper-recombination genes from the patch screen were not identified in the pinning screen, and so are false negatives. Although we have not validated the weaker hits from the pinning screen (those with recombinant frequencies between 87% and 96%), four genes in this range were validated as part of the patch screen (*APN1*, *RMI1*, *YLR235C*, and *RNH201*), 9 caused elevated levels of Rad52 foci when deleted (*APN1*, *NFI1*, *RMI1*, *POL32*, *RNH201*, *DDC1*, *HST3*, *MFT1*, and *YJR124C*) (Alvaro *et al.*, 2007; Styles *et al.*, 2016), and 3 are annotated as 'mitotic recombination increased' (*RMI1*, *DDC1*, and *HST3*; *Saccharomyces* Genome Database). Together these data suggest that additional *bona fide* hyper-recombination genes were identified in the pinning screen.

Hypo-recombination genes: By contrast to the replica-plating screen, the pinning screen detected mutants with reduced recombinant frequency, with 122 genes identified (Table 2). The genes identified were functionally diverse, with no gene ontology (GO) processes enriched. Only 19 nonessential genes are annotated as having reduced recombination as either null or hypomorphic alleles in the *Saccharomyces* genome database (SGD; accessed January 11, 2020 via YeastMine). Of these, three genes (*RAD52*, *LRP1*, and *THP1*) were detected in the pinning screen. In addition, other members of the *RAD52* epistasis group important for effective homologous recombination (*RAD50*, *RAD54* and *RAD55*) displayed a recombinant frequency lower than 33%, and *RAD51* was just above the cutoff (Table S3). Thus, our high-throughput replica-pinning approach detects mutants with very low recombinant frequencies. More generally, this observation suggests that if the pinning procedure is properly calibrated, a high-throughput replica-pinning screen is able not only to detect mutants with increased rates of a specific low-frequency event (in this case direct-repeat recombination), but also mutants with reduced rates of the same low-frequency event.

Validated hyper-recombination genes identified in both screens: We compared the genes identified in the pinning screen with those identified in the patch screen, revealing 15 genes that were identified in both screens, a statistically supported enrichment (Figure 3A; hypergeometric $P = 1.2x10^{-21}$). Combining the results of the two screens, we validated 35 genes whose deletion results in elevated spontaneous direct-repeat recombination (Table 3). Analysis of the group of 35 hyper-rec genes revealed 68 pairwise protein-protein interactions (Figure 3B), with many cases where several (if not all) members of the particular protein complex were identified. We found that 29 of the hyper-rec genes had at least one human ortholog (Table 3), indicating a high degree of conservation across the 35 validated genes. To assess the functional properties of the 35 gene hyper-rec set, we applied spatial analysis of functional enrichment (SAFE) (Baryshnikova 2016) to determine if any regions of the functional genetic interaction similarity yeast cell map (Costanzo *et al.*, 2016)
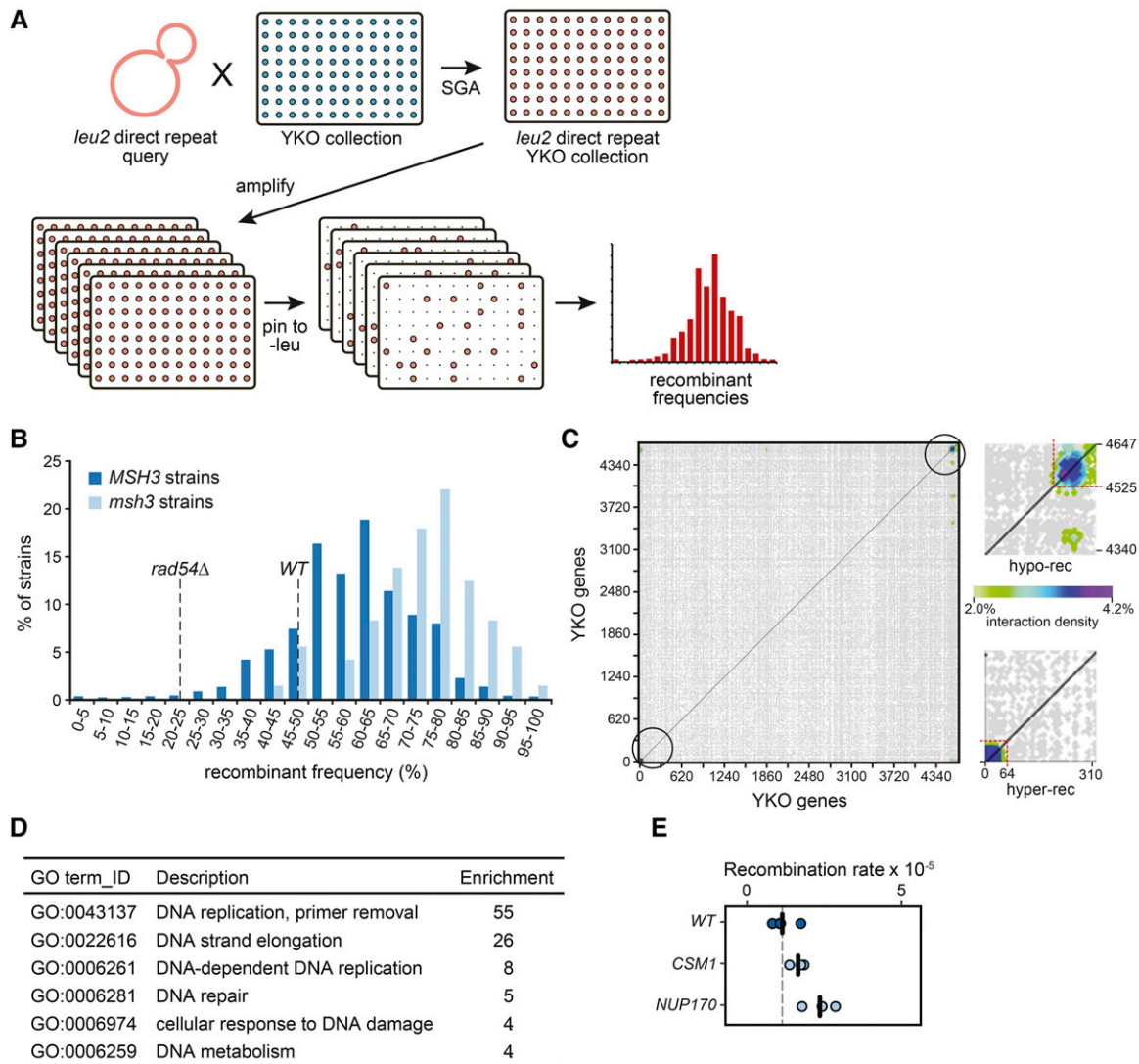
Figure 2 A high-throughput replica-pinning screen for genes controlling direct-repeat recombination. (A) Schematic representation of the screen based on high-throughput replica-pinning. The *leu2* direct-repeat recombination cassette was introduced into the yeast deletion collection as in Figure 1B. The resulting strains were amplified by parallel high-throughput replica pinning and subsequently replica-pinned to media lacking leucine to select for recombination events. Recombinant frequencies were calculated for each strain of the YKO collection. (B) Recombinant frequency distribution for the YKO collection (*MSH3* strains) and for the *msh3* strains in the collection. Recombinant frequencies for a wild-type and for a recombination-defective *rad54*Δ strain derived from a pilot experiment are indicated by the dashed lines. (C) Interaction densities determined by CLIK analysis are plotted as a two-dimensional heatmap. The cutoffs established by CLIK analysis for hyper-recombination (hyper-rec) and recombination-defective (hypo-rec) genes are shown in the insets. (D) The statistically supported GO terms enriched in the hits from the pinning assay screen are shown, with the enrichment for each term. (E) Recombination rates from fluctuation tests of *csm1*Δ and *nup170*Δ are plotted. Each data point is from an independent fluctuation test, with n = 3 for each strain. The vertical bars indicate the mean recombination rate for each strain and the wild-type data from Figure 1D are plotted for comparison.

are over-represented for the hyper-rec gene set (Figure 3C). We found a statistically supported over-representation of the hyper-rec genes in the DNA replication and repair neighborhood of the genetic interaction cell map, highlighting the importance of accurate DNA synthesis in suppressing recombination. Finally, we compared the validated hyper-rec genes to relevant functional genomic instability datasets (*Saccharomyces* Genome Database annotation, (Alvaro *et al.*, 2007; Hendry *et al.*, 2015; Stirling *et al.*, 2011; Styles *et al.*, 2016); Figure 3D). Eight of our hyper-rec genes (*HTA2*, *MSH6*, *YER188W*, *ABZ2*, *PMS1*, *MSH2*, *DFG16*, and *VMA11*) were not identified in these datasets, indicating that our screens identified

uncharacterized recombination genes. *HTA2*, *MSH6*, *PMS1*, *MSH2* have recombination phenotypes reported (see Discussion). Thus, we identify four genes without a characterized role in preventing recombination: *YER188W*, *ABZ2*, *DFG16*, and *VMA11*.

To infer gene function for the four genes lacking a characterized role in suppressing recombination, we again applied SAFE analysis (Baryshnikova 2016) to annotate the functional genetic interaction similarity yeast cell map (Costanzo *et al.*, 2016) to identify any regions that are enriched for genetic interactions with each of the four genes (Figure 4). Of particular interest, the mitochondrial functional neighborhood is enriched for negative genetic interactions with *YER188W*

■ Table 2 Hypo-recombination genes from the pinning assay screen

	Pinning Assay Hypo-Rec						
Gene name	Recombinant colonies (%)	Gene name	Recombinant colonies (%)	Gene name	Recombinant colonies (%)	Gene name	Recombinant colonies (%)
YCL021W-A	0.0	SIP3	17.2	HST4	27.1	AIM39	31.3
YEL045C	0.0	BEM1	18.8	PHO85	27.1	CIK1	31.3
GLY1	0.0	BUB3	18.8	PRM4	27.1	HOL1	31.3
HIS5	0.0	OPI3	18.8	RIM1	27.1	MET22	31.3
RAD52	2.1	YER038W-A	18.9	UBP15	27.1	SWH1	31.3
GCN4	2.9	ARG7	19.1	VMA21	27.1	RNR4	31.3
CYS4	3.1	LIN1	19.6	YBR075W	27.1	RPN4	31.3
POS5	3.1	OPY2	20.0	AAT2	27.5	RPS18B	31.3
REC104	4.2	HEF3	20.0	RAD50	27.8	TSL1	31.3
YHR080C	4.2	DAL81	20.9	ARG2	28.1	VPS60	31.3
ATP15	4.8	YLR361C-A	21.3	IRE1	28.2	VTH1	31.3
YPR099C	4.9	RPL22A	21.6	PDR16	28.2	YKE2	31.3
YOR302W	5.3	RSM7	21.7	RNR1	28.2	YNR040W	31.3
ACO2	6.4	CCR4	22.2	YKR023W	28.6	NUP84	31.6
MDM20	6.4	LOC1	22.2	ATP1	29.2	BOI1	31.7
MDM10	6.9	AHC1	22.9	FIT2	29.2	URA2	31.7
NPL3	7.1	CIN1	22.9	HSP42	29.2	RTC3	31.8
HIS7	7.7	VRP1	22.9	RAD54	29.2	THP1	31.8
FUN12	8.3	YEL014C	22.9	RAD55	29.2	BUD20	32.1
BDF1	11.1	CDC40	23.1	SNO1	29.2	RPS16A	32.6
YNL011C	12.5	MDM34	23.4	SPE2	29.2		
SWI6	12.8	OST4	23.5	SPT21	29.2		
URA1	13.2	YOL013W-B	24.0	TCD1	29.2		
YGR272C	13.2	YCK1	24.3	TPM1	29.2		
BUD19	13.3	KNH1	25.0	YDR157W	29.2		
UGO1	13.3	SHE4	25.0	YDR535C	29.2		
YBL065W	14.6	SNF6	25.0	YNL097C-A	29.2		
SWI3	14.8	YDL187C	25.0	YME1	29.6		
BRE4	15.2	LRP1	25.7	NGG1	30.3		
YGR139W	15.6	ACM1	25.9	POP2	30.4		
PMD1	15.8	VCX1	26.7	ATP11	30.8		
YHL041W	15.8	BUB1	26.8	RPL37B	31.0		
ERG28	16.7	CCW12	27.1	HFI1	31.0		
SLX5	16.7	HAM1	27.1	YML013C-A	31.1		

(Figure 4), suggesting that deletion of *YER188W* confers sensitivity to mitochondrial dysfunction. Analysis of *DFG16* revealed enrichments for positive interactions in the RIM signaling neighborhood, which is expected (Barwell *et al.*, 2005), but also for negative interactions in the DNA replication region of the map (Figure 4), indicating that *DFG16* is important for fitness when DNA replication is compromised. Analysis of *VMA11* revealed enrichment in the vesicle trafficking neighborhood, typical of vacuolar ATPase subunit genes, and analysis of *ABZ2* revealed little (Figure 4). We conclude that functional analysis suggests mechanisms by which loss of *YER188W* (oxidative stress) or *DFG16* (genome integrity) results in hyper-recombination.

DISCUSSION

We report here the first systematic, genome-wide approach to identify genes that affect direct-repeat recombination. By combining the classical patch and replica-plate method and our new replica-pinning approach, we identified many genes already implicated in homologous recombination, as well as genes with no previous connection to recombination. We failed to identify several genes known to suppress direct-repeat recombination—*e.g.*, *SRS2* and *HPR1* (Aguilera and Klein 1988)—but this is not

surprising, since most, if not all, genome-wide screens have false negatives. Here we briefly discuss the functions of the genes and complexes identified in the screens and subsequently validated by fluctuation analysis.

Mismatch repair

MLH1, *MSH2*, *MSH6* and *PMS1* are evolutionarily conserved genes involved in mismatch repair (MMR), a pathway that detects and corrects nucleotide mismatches in double-strand DNA (Spies and Fishel 2015). An anti-recombinogenic role for these four MMR genes in yeast has been previously described: specifically, MMR proteins are important to prevent homologous recombination and SSA between slightly divergent sequences, via mismatch recognition and hetero-duplex rejection (Datta *et al.*, 1996; Nicholson *et al.*, 2000; Spies and Fishel 2015; Sugawara *et al.*, 2004). The role for MMR in preventing homologous recombination is conserved also in mammalian cells (de Wind *et al.*, 1995; Elliott and Jasin 2001; Spies and Fishel 2015). It is worth noting that the presence of sequence differences between the two *leu2* alleles in the *leu2* direct-repeat assay is essential to genetically detect recombination events. Therefore, it is reasonable that this assay should detect genes involved in suppressing homologous recombination.
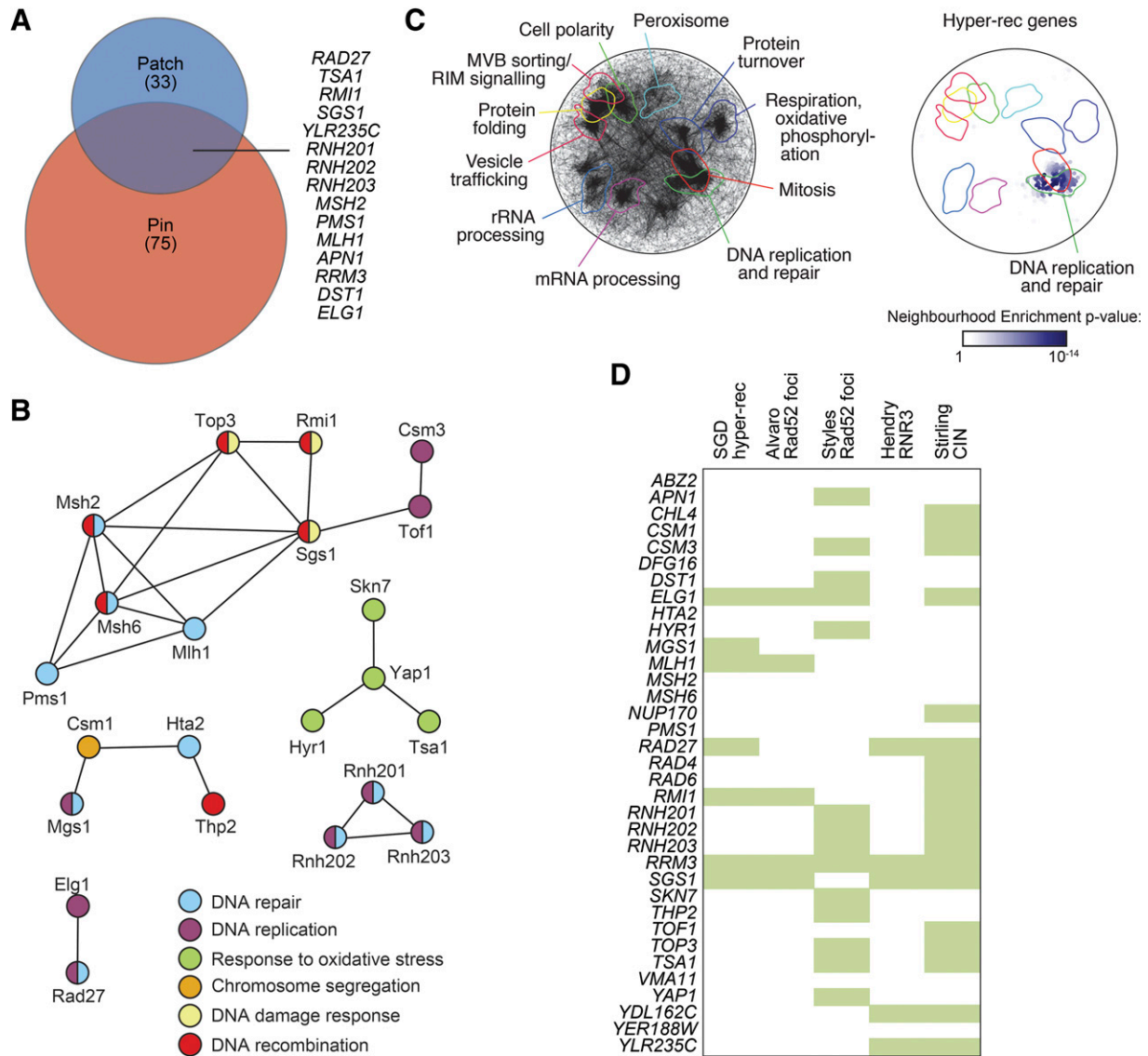
Figure 3 Functional analysis of validated hyper-rec genes. (A) The overlap of the hyper-rec genes for the two screens is plotted as a Venn diagram. The 15 genes identified in both screens are indicated. (B) A protein-protein interaction network for the proteins encoded by the 35 validated hyper-rec genes is shown. Nodes represent the proteins, and are colored to indicate function. Edges indicate a physical interaction as annotated in the GeneMania database. (C) Spatial analysis of functional enrichment. On the left, the yeast genetic interaction similarity network is annotated with GO biological process terms to identify major functional domains (Costanzo *et al.* 2016). 11 of the 17 domains are labeled and delineated by colored outlines. On the right, the network is annotated with the 35 validated hyper-rec genes. The overlay indicates the functional domains annotated on the left. Only nodes with statistically supported enrichments (SAFE score > 0.08, *P* < 0.05) are colored. (D) The 35 validated hyper-rec genes are compared with existing *Saccharomyces* Genome Database annotations and genome instability datasets that measured Rad52 focus formation (Alvaro *et al.*, 2007; Styles *et al.*, 2016), *RNR3* induction (Hendry *et al.*, 2015), or chromosome instability (CIN; (Stirling *et al.*, 2011)). A green bar indicates that the gene has the given annotation or was detected in the indicated screen.

Sgs1-Top3-Rmi1 complex

The evolutionarily conserved helicase-topoisomerase complex Sgs1-Top3-Rmi1 is involved in DSB resection and in dissolution of recombination intermediates (Symington *et al.*, 2014). Consistent with previous observations (Chang *et al.*, 2005), our screen identified all three members of the complex, together with *YLR235C*, a dubious ORF that overlaps the *TOP3* gene. The Sgs1-Top3-Rmi1 complex dissolves double Holliday junction structures to prevent crossover formation (Cejka *et al.*, 2010). The same role has been reported for BLM helicase, the human Sgs1 homolog mutated in the genome stability disorder Bloom syndrome (Wu *et al.*, 2006; Yang *et al.*,

2010). Furthermore, several genetic studies indicate that the anti-recombinogenic activity of Sgs1-Top3-Rmi1 cooperates with MMR proteins in heteroduplex rejection to prevent homeologous recombination (Chakraborty *et al.*, 2016; Goldfarb and Alani 2005; Myung *et al.*, 2001; Spell and Jinks-Robertson 2004; Sugawara *et al.*, 2004).

MGS1

In our screen we also identified *MGS1*, the homolog of the WRN-interacting protein WRNIP1. Mgs1 displays DNA-dependent ATPase and DNA strand annealing activities. Deletion of *MGS1* causes

Gene name	Description	Human ortholog(s)
HTA2	Histone H2A	H2A
NUP170	Subunit of inner ring of nuclear pore complex	NUP155
CSM1	Nucleolar protein that mediates homolog segregation during meiosis I	
YDL162C	Dubious open reading frame; overlaps the CDC9 promoter	LIG1
MSH6	Protein required for mismatch repair in mitosis and meiosis	MSH6
CHL4	Outer kinetochore protein required for chromosome stability	CENPN
RNH202	Ribonuclease H2 subunit	RNASEH2B
RAD4	Protein that recognizes and binds damaged DNA during NER	XPC
YER188W	Putative protein of unknown function	
DST1	General transcription elongation factor TFIIS	TCEA1, TCEA2, TCEA3
RAD6	Ubiquitin-conjugating enzyme	UBE2A, UBE2B
RRM3	DNA helicase involved in rDNA replication and Ty1 transposition	PIF1
THP2	Subunit of the THO and TREX complexes	
SKN7	Nuclear response regulator and transcription factor	HSF1, HSF2, HSF4, HSF5
HYR1	Thiol peroxidase	GPX1, GPX2, GPX3, GPX4, GPX5, GPX6, GPX7
RAD27	5′ to 3′ exonuclease, 5′ flap endonuclease	FEN1
APN1	Major apurinic/apyrimidinic endonuclease	APE1
RNH203	Ribonuclease H2 subunit	RNASEH2C
TOP3	DNA Topoisomerase III	TOP3A
YLR235C	Dubious open reading frame; overlaps the TOP3 gene	TOP3A
YAP1	Basic leucine zipper transcription factor	
TSA1	Thioredoxin peroxidase	PRDX1, PRDX2, PRDX3, PRDX4
CSM3	Replication fork associated factor	TIPIN
MLH1	Protein required for mismatch repair in mitosis and meiosis	MLH1
SGS1	RecQ family nucleolar DNA helicase	BLM
ABZ2	Aminodeoxychorismate lyase (4-amino-4-deoxychorismate lyase)	
RNH201	Ribonuclease H2 catalytic subunit	RNASEH2A
PMS1	ATP-binding protein required for mismatch repair	PMS1
MGS1	Protein with DNA-dependent ATPase and ssDNA annealing activities	WRNIP1
TOF1	Subunit of a replication-pausing checkpoint complex	TIMELESS
MSH2	Protein that binds to DNA mismatches	MSH2
DFG16	Probable multiple transmembrane protein	
ELG1	Subunit of an alternative replication factor C complex	ATAD5
RMI1	Subunit of the RecQ (Sgs1) - Topo III (Top3) complex	RMI1
VMA11	Vacuolar ATPase V0 domain subunit c′	ATP6VOC

hyper-recombination, including elevated direct-repeat recombination (Hishida *et al.*, 2001). It seems that Mgs1 promotes faithful DNA replication by regulating Polδ, and promoting replication fork restart after stalling (Branzei *et al.*, 2002; Saugar *et al.*, 2012). The absence of Mgs1 could result in increased replication fork collapse, leading to the formation of recombinogenic DSBs (Branzei *et al.*, 2002). Similar roles have been suggested for WRNIP1 in mammalian cells (Leuzzi *et al.*, 2016; Tsurimoto *et al.*, 2005).

RNase H2 complex

RNH201 encodes the evolutionarily conserved catalytic subunit of RNase H2, while the two non-catalytic subunits are encoded by RNH202 and RNH203 genes. This enzyme cleaves the RNA moiety in RNA-DNA hybrids originating from Okazaki fragments, co-transcriptional R-loops, and ribonucleotide incorporation by replicative polymerases (Cerritelli and Crouch 2009). Deletion of any of the three subunits in yeast inactivates the whole complex. Human RNase H2 genes are mutated in Aicardi-Goutières syndrome, a severe neurological disorder (Crow *et al.*, 2006). Inactivation of yeast RNase H2 causes elevated LOH, ectopic recombination and direct-repeat recombination (Conover *et al.*, 2015; Potenski *et al.*, 2014), mostly dependent on Top1 activity. What is the recombinogenic intermediate accumulated in the absence of RNase H2? It has been suggested

that Top1-dependent cleavage at the ribonucleotide site creates a nick that can be further converted into a recombinogenic DSB (Potenski *et al.*, 2014). Recent genetic studies indicate that, while in the case of LOH events hyper-recombination is caused by Top1-dependent processing of single ribonucleotides incorporated by leading strand polymerases and/or by accumulation of recombinogenic R-loops (Conover *et al.*, 2015; Cornelio *et al.*, 2017; Keskin *et al.*, 2014; O'Connell *et al.*, 2015), elevated direct-repeat recombination results instead from Top1-dependent cleavage of stretches of ribonucleotides, resulting from defective R-loop removal or Okazaki fragment processing in the absence of RNase H2 (Epshtein *et al.*, 2016). In line with this model, we also detected elevated direct-repeat recombination rate in the absence of the Thp2 member of the THO complex, which functions at the interface between transcription and mRNA export to prevent R-loop accumulation (Chavez *et al.*, 2000; Huertas and Aguilera 2003), DST1, which encodes a transcription elongation factor and is anti-recombinogenic (Owiti *et al.*, 2017), and the flap endonuclease encoded by RAD27, which is involved in Okazaki fragment processing (Balakrishnan and Bambara 2013) (Table 3). Furthermore, deletion of the dubious ORF YDL162C, also identified in our screen, likely affects the expression level of neighboring CDC9, an essential gene encoding DNA Ligase I, involved in Okazaki fragment processing and ligation after ribonucleotide removal from DNA. Together, available data suggest that different modes
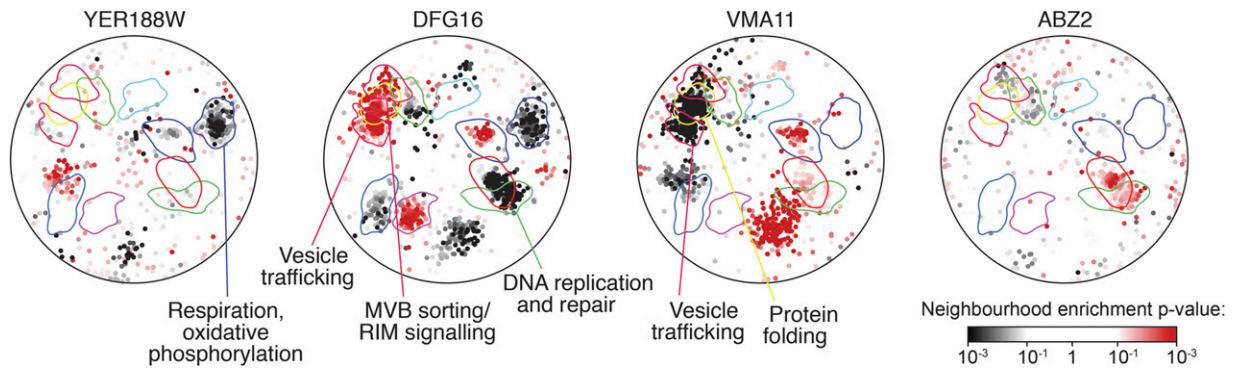
Figure 4 Spatial analysis of functional enrichment for four hyper-rec genes. The genetic interactions of each of the indicated genes was tested for enrichments in the functional neighborhoods of the yeast genetic interaction similarity network. The overlay indicates a subset of functional domains as annotated on Figure 3C. Nodes with statistically supported enrichments (Neighborhood enrichment $P < 0.05$) are colored, black for negative genetic interactions and red for positive genetic interactions.

leading to accumulation of RNA-DNA hybrids or unprocessed Okazaki fragments result in hyper-recombination.

Fork protection complex

Tof1 and Csm3 (Timeless and Tipin in human cells) form the fork protection complex (FPC), involved in stabilization of replication forks, maintenance of sister chromatid cohesion and DNA replication checkpoint signaling (Bando *et al.*, 2009; Chou and Elledge 2006; Katou *et al.*, 2003; Leman *et al.*, 2010; Mayer *et al.*, 2004; Mohanty *et al.*, 2006; Noguchi *et al.*, 2004, 2003; Xu *et al.*, 2004). Recently, Tof1 and Csm3 were implicated in restricting fork rotation genome-wide during replication; they perform this role independently of their interacting partner Mrc1, which we did not identify in our screen (Schalbetter *et al.*, 2015). In the absence of Tof1 or Csm3, excessive fork rotation can cause spontaneous DNA damage, in the form of recombinogenic ssDNA and DSBs (Chou and Elledge 2006; Schalbetter *et al.*, 2015; Sommariva *et al.*, 2005; Urtishak *et al.*, 2009). Indeed, depletion of Tof1 and Csm3 orthologs results in accumulation of recombination intermediates in fission yeast and mouse cells (Noguchi *et al.*, 2004, 2003; Sommariva *et al.*, 2005; Urtishak *et al.*, 2009).

RRM3

The *RRM3* gene, encoding a 5′ to 3′ DNA helicase, was initially identified because its absence causes hyper-recombination between endogenous tandem-repeated sequences (such as the rDNA locus and the *CUP1* genes) (Keil and McWilliams 1993). The Rrm3 helicase travels with the replication fork and facilitates replication through genomic sites containing protein-DNA complexes that, in its absence, cause replication fork stalling and breakage. Such Rrm3-dependent sites include the rDNA, telomeres, tRNA genes, inactive replication origins, centromeres, and the silent mating-type loci (Azvolinsky *et al.*, 2006; Ivessa *et al.*, 2003, 2000; Schmidt and Kolodner 2004; Torres *et al.*, 2004). Intriguingly, a tRNA gene is located about 350 bp upstream the chromosomal location of the *leu2* direct-repeat recombination marker. Increased replication fork pausing in the absence of Rrm3 could cause recombinogenic DSBs, explaining the elevated direct-repeat recombination we observe in the *rrm3Δ* strain.

Oxidative stress response genes

YAP1 and *SKN7* encode two transcription factors important for the activation of the cellular response to oxidative stress (Morano *et al.*, 2012). The glutathione peroxidase encoded by *HYR1* has a major role in activating Yap1 in response to oxidative stress (Delaunay *et al.*, 2002).

TSA1 is a Yap1 and Skn7 target and encodes a peroxiredoxin that scavenges endogenous hydrogen peroxide (Wong *et al.*, 2004). Deletion of *TSA1* causes hyper-recombination between inverted repeats (Huang and Kolodner 2005), and oxidative stress response genes (including *TSA1*, *SKN7* and *YAP1*) are synthetic sick or lethal with HR mutants (Pan *et al.*, 2006; Yi *et al.*, 2016). A likely explanation for the elevated direct-repeat recombination we measured in strains defective for the oxidative stress response, therefore, is that oxidative DNA damage generates replication blocking lesions and/or replication-associated DSBs, both of which are processed by the HR pathway (Huang and Kolodner 2005). An alternative explanation could be that extensive oxidative DNA damage results in the saturation of the mismatch-binding step of MMR, compromising MMR-dependent heteroduplex rejection, resulting in increased homeologous recombination (Hum and Jinks-Robertson 2018; Spies and Fishel 2015).

Other DNA repair genes

APN1 encodes the main apurinic/apyrimidinic (AP) endonuclease involved in yeast base excision repair (BER). Removal of endogenous alkylating damage can generate abasic sites, which are mostly processed by Apn1 (Boiteux and Guillet 2004; Popoff *et al.*, 1990; Xiao and Samson 1993). In the absence of *APN1*, abasic sites accumulate, which can hamper DNA replication. The recombination pathway is involved in the repair and/or bypass of these abasic sites, as suggested by the genetic interactions between the BER and the HR pathways (Boiteux and Guillet 2004; Swanson *et al.*, 1999; Vance and Wilson 2001). The *APN1* gene is adjacent to *RAD27*, and therefore it is also possible that the hyper-recombination phenotype of *apn1Δ* is due to a "neighbouring-gene effect" on *RAD27*, as was reported in the case of telomere length alteration (Ben-Shitrit *et al.*, 2012).

HTA2, which encodes one copy of histone H2A, is of course important for appropriate nucleosome assembly. Reducing histone levels by deleting one H3-H4 gene pair or by partial depletion of H4 increases recombination (Clemente-Ruiz and Prado 2009; Liang *et al.*, 2012; Prado and Aguilera 2005), and it is likely that reducing *HTA2* gene dosage also does so. Since histone depletion results in diverse chromatin defects, the exact mechanisms by which recombination is induced are elusive.

RAD4 encodes a key factor of nucleotide excision repair (NER), and is involved in direct recognition and binding of DNA damage (Prakash and Prakash 2000), while *RAD6* is a key gene controlling the post replication repair (PRR) DNA damage tolerance pathway (Ulrich 2005). Genetic studies suggest that BER, NER, PRR and HR

can redundantly process spontaneous DNA lesions, and inactivation of one pathway shifts the burden on the others. This mechanism could explain why deletion of *RAD4* or *RAD6* causes a modest increase in spontaneous direct-repeat recombination (Swanson *et al.*, 1999).

CSM1 encodes a nucleolar protein that serves as a kinetochore organizer to promote chromosome segregation in meiosis, and is involved in localization and silencing of rDNA and telomeres in mitotic cells (Poon and Mekhail 2011). Interestingly, Csm1 is important to inhibit homologous recombination at the rDNA locus and other repeated sequences (Burrack *et al.*, 2013; Huang *et al.*, 2006; Mekhail *et al.*, 2008). The nuclear pore complex has an intimate connection to recombination, in that some DSBs move to and are likely repaired at the NPC (Freudenreich and Su 2016). The NPC gene *NUP170* has not been directly implicated in DSB repair, but is important for chromosome segregation (Kerscher *et al.*, 2001).

The unknowns (YER188W, ABZ2, DFG16, and VMA11)

Unexpectedly, the top hyper-rec gene identified in our screen is *VMA11*, which encodes a subunit of the evolutionarily conserved vacuolar H⁺-ATPase (V-ATPase), important for vacuole acidification and cellular pH regulation (Hirata *et al.*, 1997; Kane 2006; Umemoto *et al.*, 1991). *VMA11* involvement in genome maintenance is suggested by the sensitivity of a *vma11Δ* strain to several genotoxic agents, namely doxorubicin, ionizing radiation, cisplatin and oxidative stress (Thorpe *et al.*, 2004; Xia *et al.*, 2007). V-ATPase defects in yeast result in endogenous oxidative stress and defective Fe/S cluster biogenesis as a consequence of mitochondrial depolarization (Hughes and Gottschling 2012; Milgrom *et al.*, 2007; Veatch *et al.*, 2009). Of note, several DNA replication and repair factors are Fe/S cluster proteins (Veatch *et al.*, 2009; Zhang 2014). Therefore, the hyper-recombination phenotype of *vma11Δ* could be due to increased spontaneous DNA damage, caused by elevated endogenous oxidative stress and/or by defective DNA replication and repair as a consequence of compromised Fe/S cluster biogenesis. However, *VMA11* was not detected in screens for increased Rad52 foci (Alvaro *et al.*, 2007; Styles *et al.*, 2016), or in a screen for increased DNA damage checkpoint activation (Hendry *et al.*, 2015), suggesting that spontaneous DNA damage might not accumulate to high levels in *vma11Δ*.

ABZ2 encodes an enzyme involved in folate biosynthesis (Botet *et al.*, 2007). Folate deficiency and the resulting compromise of nucleotide synthesis could promote recombination, although yeast culture media are rich in folate, and the *ABZ2* genetic interaction profile reveals no similarity to nucleotide biosynthesis genes (Usaj *et al.*, 2017). *DFG16* encodes a predicted transmembrane protein involved in pH sensing (Barwell *et al.*, 2005). Interestingly, SAFE analysis indicates a role for *DFG16* in DNA replication and/or DNA repair, in addition to the expected role in pH signaling. There is currently little insight into the function of *YER188W*. SAFE analysis indicates a possible role in mitochondrial function, however a protein product of *YER188W* has not been detected to date in either mass spectrometry or GFP fusion protein analyses (Breker *et al.*, 2014; Ho *et al.*, 2018; Huh *et al.*, 2003).

In summary, despite direct-repeat recombination having been studied for decades, with our combined screening approach we were able to identify novel genes that affect this process, several of which are evolutionarily conserved. Since repeated sequences are abundant in mammalian genomes, our findings might be important for future studies on recombination and genome integrity in human cells. In addition, our high-throughput screening approach will likely be useful to study other cellular processes that occur at low frequency.

LITERATURE CITED

Aguilera, A., and T. García-Muse, 2013 Causes of genome instability. Annu. Rev. Genet. 47: 1–32. https://doi.org/10.1146/annurev-genet-111212-133232

Aguilera, A., and H. L. Klein, 1988 Genetic control of intrachromosomal recombination in *Saccharomyces cerevisiae*. I. Isolation and genetic characterization of hyper-recombination mutations. Genetics 119: 779–790. https://www.genetics.org/content/119/4/779.long

Alvaro, D., M. Lisby, and R. Rothstein, 2007 Genome-wide analysis of Rad52 foci reveals diverse mechanisms impacting recombination. PLoS Genet. 3: e228. https://doi.org/10.1371/journal.pgen.0030228

Andersen, M. P., Z. W. Nelson, E. D. Hetrick, and D. E. Gottschling, 2008 A genetic screen for increased loss of heterozygosity in *Saccharomyces cerevisiae*. Genetics 179: 1179–1195. https://doi.org/10.1534/genetics.108.089250

Azvolinsky, A., S. Dunaway, J. Z. Torres, J. B. Bessler, and V. A. Zakian, 2006 The *S. cerevisiae* Rrm3p DNA helicase moves with the replication fork and affects replication of all yeast chromosomes. Genes Dev. 20: 3104–3116. https://doi.org/10.1101/gad.1478906

Balakrishnan, L., and R. A. Bambara, 2013 Flap Endonuclease 1. Annu. Rev. Biochem. 82: 119–138. https://doi.org/10.1146/annurev-biochem-072511-122603

Bando, M., Y. Katou, M. Komata, H. Tanaka, T. Itoh *et al.*, 2009 Csm3, Tof1, and Mrc1 form a heterotrimeric mediator complex that associates with DNA replication forks. J. Biol. Chem. 284: 34355–34365. https://doi.org/10.1074/jbc.M109.065730

Barwell, K. J., J. H. Boysen, W. Xu, and A. P. Mitchell, 2005 Relationship of *DFG16* to the Rim101p pH response pathway in *Saccharomyces cerevisiae* and *Candida albicans*. Eukaryot. Cell 4: 890–899. https://doi.org/10.1128/EC.4.5.890-899.2005

Baryshnikova, A., 2016 Systematic functional annotation and visualization of biological networks. Cell Syst. 2: 412–421. https://doi.org/10.1016/j.cels.2016.04.014

Bellaoui, M., M. Chang, J. Ou, H. Xu, C. Boone *et al.*, 2003 Elg1 forms an alternative RFC complex important for DNA replication and genome integrity. EMBO J. 22: 4304–4313. https://doi.org/10.1093/emboj/cdg406

Ben-Aroya, S., A. Koren, B. Liefshitz, R. Steinlauf, and M. Kupiec, 2003 *ELG1*, a yeast gene required for genome stability, forms a complex related to replication factor C. Proc. Natl. Acad. Sci. USA 100: 9906–9911. https://doi.org/10.1073/pnas.1633757100

Ben-Shitrit, T., N. Yosef, K. Shemesh, R. Sharan, E. Ruppin *et al.*, 2012 Systematic identification of gene annotation errors in the widely used yeast mutation collections. Nat. Methods 9: 373–378. https://doi.org/10.1038/nmeth.1890

Boiteux, S., and M. Guillet, 2004 Abasic sites in DNA: Repair and biological consequences in *Saccharomyces cerevisiae*. DNA Repair (Amst.) 3: 1–12. https://doi.org/10.1016/j.dnarep.2003.10.002

Botet, J., L. Mateos, J. L. Revuelta, and M. A. Santos, 2007 A chemogenomic screening of sulfanilamide-hypersensitive *Saccharomyces cerevisiae* mutants uncovers *ABZ2*, the gene encoding a fungal aminodeoxychorismate lyase. Eukaryot. Cell 6: 2102–2111. https://doi.org/10.1128/EC.00266-07

Brachmann, C. B., A. Davies, G. J. Cost, E. Caputo, J. Li *et al.*, 1998 Designer deletion strains derived from *Saccharomyces cerevisiae* S288C: a useful set

of strains and plasmids for PCR-mediated gene disruption and other applications. Yeast 14: 115–132. https://doi.org/10.1002/(SICI)1097-0061(19980130)14:2<115::AID-YEA204>3.0.CO;2-2

Branzei, D., M. Seki, F. Onoda, and T. Enomoto, 2002   The product of *Saccharomyces cerevisiae WHIP/MGS1*, a gene related to replication factor C genes, interacts functionally with DNA polymerase delta. Mol. Genet. Genomics 268: 371–386. https://doi.org/10.1007/s00438-002-0757-3

Breker, M., M. Gymrek, O. Moldavski, and M. Schuldiner, 2014   LoQAtE--Localization and Quantitation ATlas of the yeast proteomE. A new tool for multiparametric dissection of single-protein behavior in response to biological perturbations in yeast. Nucleic Acids Res. 42: D726–D730. https://doi.org/10.1093/nar/gkt933

Burrack, L. S., S. E. Applen Clancey, J. M. Chacon, M. K. Gardner, and J. Berman, 2013   Monopolin recruits condensin to organize centromere DNA and repetitive DNA sequences. Mol. Biol. Cell 24: 2807–2819. https://doi.org/10.1091/mbc.e13-05-0229

Cejka, P., J. L. Plank, C. Z. Bachrati, I. D. Hickson, and S. C. Kowalczykowski, 2010   Rmi1 stimulates decatenation of double Holliday junctions during dissolution by Sgs1-Top3. Nat. Struct. Mol. Biol. 17: 1377–1382. https://doi.org/10.1038/nsmb.1919

Cerritelli, S. M., and R. J. Crouch, 2009   Ribonuclease H: the enzymes in eukaryotes. FEBS J. 276: 1494–1505. https://doi.org/10.1111/j.1742-4658.2009.06908.x

Chakraborty, U., C. M. George, A. M. Lyndaker, and E. Alani, 2016   A delicate balance between repair and replication factors regulates recombination between divergent DNA sequences in *Saccharomyces cerevisiae*. Genetics 202: 525–540. https://doi.org/10.1534/genetics.115.184093

Chang, M., M. Bellaoui, C. Zhang, R. Desai, P. Morozov *et al.*, 2005   *RMI1/NCE4*, a suppressor of genome instability, encodes a member of the RecQ helicase/Topo III complex. EMBO J. 24: 2024–2033. https://doi.org/10.1038/sj.emboj.7600684

Chavez, S., T. Beilharz, A. G. Rondón, H. Erdjument-Bromage, P. Tempst *et al.*, 2000   A protein complex containing Tho2, Hpr1, Mft1 and a novel protein, Thp2, connects transcription elongation with mitotic recombination in *Saccharomyces cerevisiae*. EMBO J. 19: 5824–5834. https://doi.org/10.1093/emboj/19.21.5824

Chou, D. M., and S. J. Elledge, 2006   Tipin and Timeless form a mutually protective complex required for genotoxic stress resistance and checkpoint function. Proc. Natl. Acad. Sci. USA 103: 18143–18147. https://doi.org/10.1073/pnas.0609251103

Claussin, C., and M. Chang, 2015   The many facets of homologous recombination at telomeres. Microb. Cell 2: 308–321. https://doi.org/10.15698/mic2015.09.224

Claussin, C., D. Porubský, D. C. J. Spierings, N. Halsema, S. Rentas *et al.*, 2017   Genome-wide mapping of sister chromatid exchange events in single yeast cells using strand-seq. eLife 6: e30560. https://doi.org/10.7554/eLife.30560

Clemente-Ruiz, M., and F. Prado, 2009   Chromatin assembly controls replication fork stability. EMBO Rep. 10: 790–796. https://doi.org/10.1038/embor.2009.67

Conover, H. N., S. A. Lujan, M. J. Chapman, D. A. Cornelio, R. Sharif *et al.*, 2015   Stimulation of chromosomal rearrangements by ribonucleotides. Genetics 201: 951–961. https://doi.org/10.1534/genetics.115.181149

Cornelio, D. A., H. N. C. Sedam, J. A. Ferrarezi, N. M. V. Sampaio, and J. L. Argueso, 2017   Both R-loop removal and ribonucleotide excision repair activities of RNase H2 contribute substantially to chromosome stability. DNA Repair (Amst.) 52: 110–114. https://doi.org/10.1016/j.dnarep.2017.02.012

Costanzo, M., B. VanderSluis, E. N. Koch, A. Baryshnikova, C. Pons *et al.*, 2016   A global genetic interaction network maps a wiring diagram of cellular function. Science 353: aaf1420. https://doi.org/10.1126/science.aaf1420

Crow, Y. J., A. Leitch, B. E. Hayward, A. Garner, R. Parmar *et al.*, 2006   Mutations in genes encoding ribonuclease H2 subunits cause

Aicardi-Goutières syndrome and mimic congenital viral brain infection. Nat. Genet. 38: 910–916. https://doi.org/10.1038/ng1842

Datta, A., A. Adjiri, L. New, G. F. Crouse, and S. Jinks Robertson, 1996   Mitotic crossovers between diverged sequences are regulated by mismatch repair proteins in *Saccharomyces cerevisiae*. Mol. Cell. Biol. 16: 1085–1093. https://doi.org/10.1128/MCB.16.3.1085

de Wind, N., M. Dekker, A. Berns, M. Radman, and H. te Riele, 1995   Inactivation of the mouse Msh2 gene results in mismatch repair deficiency, methylation tolerance, hyperrecombination, and predisposition to cancer. Cell 82: 321–330. https://doi.org/10.1016/0092-8674(95)90319-4

Delaunay, A., D. Pflieger, M.-B. Barrault, J. Vinh, and M. B. Toledano, 2002   A thiol peroxidase is an H_2O_2 receptor and redox-transducer in gene activation. Cell 111: 471–481. https://doi.org/10.1016/S0092-8674(02)01048-6

Dittmar, J. C., S. Pierce, R. Rothstein, and R. J. D. Reid, 2013   Physical and genetic-interaction density reveals functional organization and informs significance cutoffs in genome-wide screens. Proc. Natl. Acad. Sci. USA 110: 7389–7394. https://doi.org/10.1073/pnas.1219582110

Dittmar, J. C., R. J. D. Reid, and R. Rothstein, 2010   ScreenMill: a freely available software suite for growth measurement, analysis and visualization of high-throughput screen data. BMC Bioinformatics 11: 353. https://doi.org/10.1186/1471-2105-11-353

Elliott, B., and M. Jasin, 2001   Repair of double-strand breaks by homologous recombination in mismatch repair-defective mammalian cells. Mol. Cell. Biol. 21: 2671–2682. https://doi.org/10.1128/MCB.21.8.2671-2682.2001

Epshtein, A., C. Potenski, and H. Klein, 2016   Increased spontaneous recombination in RNase H2- deficient cells arises from multiple contiguous rNMPs and not from single rNMP residues incorporated by DNA polymerase epsilon. Microb. Cell 3: 248–254. https://doi.org/10.15698/mic2016.06.506

Freudenreich, C. H., and X. A. Su, 2016   Relocalization of DNA lesions to the nuclear pore complex. FEMS Yeast Res. 16: fow095. https://doi.org/10.1093/femsyr/fow095

George, C. M., and E. Alani, 2012   Multiple cellular mechanisms prevent chromosomal rearrangements involving repetitive DNA. Crit. Rev. Biochem. Mol. Biol. 47: 297–313. https://doi.org/10.3109/10409238.2012.675644

Giaever, G., A. M. Chu, L. Ni, C. Connelly, L. Riles *et al.*, 2002   Functional profiling of the *Saccharomyces cerevisiae* genome. Nature 418: 387–391. https://doi.org/10.1038/nature00935

Goldfarb, T., and E. Alani, 2005   Distinct roles for the *Saccharomyces cerevisiae* mismatch repair proteins in heteroduplex rejection, mismatch repair and nonhomologous tail removal. Genetics 169: 563–574. https://doi.org/10.1534/genetics.104.035204

Hendry, J. A., G. Tan, J. Ou, C. Boone, and G. W. Brown, 2015   Leveraging DNA damage response signaling to identify yeast genes controlling genome stability. G3 (Bethesda) 5: 997–1006. https://doi.org/10.1534/g3.115.016576

Heyer, W. D., 2015   Regulation of recombination and genomic maintenance. Cold Spring Harb. Perspect. Biol. 7: a016501. https://doi.org/10.1101/cshperspect.a016501

Hirata, R., L. A. Graham, A. Takatsuki, T. H. Stevens, and Y. Anraku, 1997   *VMA11* and *VMA16* encode second and third proteolipid subunits of the *Saccharomyces cerevisiae* vacuolar membrane H^+-ATPase. J. Biol. Chem. 272: 4795–4803. https://doi.org/10.1074/jbc.272.8.4795

Hishida, T., H. Iwasaki, T. Ohno, T. Morishita, and H. Shinagawa, 2001   A yeast gene, *MGS1*, encoding a DNA-dependent AAA+ ATPase is required to maintain genome stability. Proc. Natl. Acad. Sci. USA 98: 8283–8289. https://doi.org/10.1073/pnas.121009098

Ho, B., A. Baryshnikova, and G. W. Brown, 2018   Unification of protein abundance datasets yields a quantitative *Saccharomyces cerevisiae* proteome. Cell Syst. 6: 192–205. https://doi.org/10.1016/j.cels.2017.12.004

Huang, J., I. L. Brito, J. Villén, S. P. Gygi, A. Amon *et al.*, 2006   Inhibition of homologous recombination by a cohesin-associated clamp complex

recruited to the rDNA recombination enhancer. Genes Dev. 20: 2887–2901. https://doi.org/10.1101/gad.1472706

Huang, M.-E., and R. D. Kolodner, 2005   A biological network in *Saccharomyces cerevisiae* prevents the deleterious effects of endogenous oxidative DNA damage. Mol. Cell 17: 709–720. https://doi.org/10.1016/j.molcel.2005.02.008

Huertas, P., and A. Aguilera, 2003   Cotranscriptionally formed DNA:RNA hybrids mediate transcription elongation impairment and transcription-associated recombination. Mol. Cell 12: 711–721. https://doi.org/10.1016/j.molcel.2003.08.010

Hughes, A. L., and D. E. Gottschling, 2012   An early age increase in vacuolar pH limits mitochondrial function and lifespan in yeast. Nature 492: 261–265. https://doi.org/10.1038/nature11654

Huh, W.-K., J. V. Falvo, L. C. Gerke, A. S. Carroll, R. W. Howson *et al.*, 2003   Global analysis of protein localization in budding yeast. Nature 425: 686–691. https://doi.org/10.1038/nature02026

Hum, Y. F., and S. Jinks-Robertson, 2018   DNA strand-exchange patterns associated with double-strand break-induced and spontaneous mitotic crossovers in *Saccharomyces cerevisiae*. PLoS Genet. 14: e1007302. https://doi.org/10.1371/journal.pgen.1007302

Hunter, N., 2015   Meiotic recombination: The essence of heredity. Cold Spring Harb. Perspect. Biol. 7: a016618. https://doi.org/10.1101/cshperspect.a016618

Ivessa, A. S., B. A. Lenzmeier, J. B. Bessler, L. K. Goudsouzian, S. L. Schnakenberg *et al.*, 2003   The *Saccharomyces cerevisiae* helicase Rrm3p facilitates replication past nonhistone protein-DNA complexes. Mol. Cell 12: 1525–1536. https://doi.org/10.1016/S1097-2765(03)00456-8

Ivessa, A. S., J. Q. Zhou, and V. A. Zakian, 2000   The *Saccharomyces* Pif1p DNA helicase and the highly related Rrm3p have opposite effects on replication fork progression in ribosomal DNA. Cell 100: 479–489. https://doi.org/10.1016/S0092-8674(00)80683-2

Johnson, R. D., and M. Jasin, 2000   Sister chromatid gene conversion is a prominent double-strand break repair pathway in mammalian cells. EMBO J. 19: 3398–3407. https://doi.org/10.1093/emboj/19.13.3398

Kadyk, L. C., and L. H. Hartwell, 1992   Sister chromatids are preferred over homologs as substrates for recombinational repair in *Saccharomyces cerevisiae*. Genetics 132: 387–402. https://www.genetics.org/content/132/2/387.long

Kane, P. M., 2006   The where, when, and how of organelle acidification by the yeast vacuolar H⁺-ATPase. Microbiol. Mol. Biol. Rev. 70: 177–191. https://doi.org/10.1128/MMBR.70.1.177-191.2006

Katou, Y., Y. Kanoh, M. Bando, H. Noguchi, H. Tanaka *et al.*, 2003   S-phase checkpoint proteins Tof1 and Mrc1 form a stable replication-pausing complex. Nature 424: 1078–1083. https://doi.org/10.1038/nature01900

Keil, R. L., and A. D. McWilliams, 1993   A gene with specific and global effects on recombination of sequences from tandemly repeated genes in *Saccharomyces cerevisiae*. Genetics 135: 711–718. https://doi.org/10.1016/0168–9525(94)90142–2

Kerscher, O., P. Hieter, M. Winey, and M. A. Basrai, 2001   Novel role for a *Saccharomyces cerevisiae* nucleoporin, Nup170p, in chromosome segregation. Genetics 157: 1543–1553. https://www.genetics.org/content/157/4/1543.long

Keskin, H., Y. Shen, F. Huang, M. Patel, T. Yang *et al.*, 2014   Transcript-RNA-templated DNA recombination and repair. Nature 515: 436–439. https://doi.org/10.1038/nature13682

Krejci, L., V. Altmannova, M. Spirek, and X. Zhao, 2012   Homologous recombination and its regulation. Nucleic Acids Res. 40: 5795–5818. https://doi.org/10.1093/nar/gks270

Kuzmin, E., M. Costanzo, B. Andrews, and C. Boone, 2016   Synthetic genetic array analysis. Cold Spring Harb. Protoc. 2016: pdb.prot088807. https://doi.org/10.1101/pdb.prot088807

Lea, D. E., and C. A. Coulson, 1949   The distribution of the numbers of mutants in bacterial populations. J. Genet. 49: 264–285. https://doi.org/10.1007/BF02986080

Lehner, K. R., M. M. Stone, R. A. Farber, and T. D. Petes, 2007   Ninety-six haploid yeast strains with individual disruptions of Open Reading Frames between *YOR097C* and *YOR192C*, constructed for the *Saccharomyces*

Genome Deletion Project, have an additional mutation in the mismatch repair gene *MSH3*. Genetics 177: 1951–1953. https://doi.org/10.1534/genetics.107.079368

Leman, A. R., C. Noguchi, C. Y. Lee, and E. Noguchi, 2010   Human Timeless and Tipin stabilize replication forks and facilitate sister-chromatid cohesion. J. Cell Sci. 123: 660–670. https://doi.org/10.1242/jcs.057984

Leuzzi, G., V. Marabitti, P. Pichierri, and A. Franchitto, 2016   WRNIP1 protects stalled forks from degradation and promotes fork restart after replication stress. EMBO J. 35: 1437–1451. https://doi.org/10.15252/embj.201593265

Liang, D., S. L. Burkhart, R. K. Singh, M. H. M. Kabbaj, and A. Gunjan, 2012   Histone dosage regulates DNA damage sensitivity in a checkpoint-independent manner by the homologous recombination pathway. Nucleic Acids Res. 40: 9604–9620. https://doi.org/10.1093/nar/gks722

López-Flores, I., and M. A. Garrido-Ramos, 2012   The repetitive DNA content of eukaryotic genomes. Genome Dyn. 7: 1–28. https://doi.org/10.1159/000337118

Luria, S. E., and M. Delbrück, 1943   Mutations of bacteria from virus sensitivity to virus resistance. Genetics 28: 491–511. https://www.genetics.org/content/28/6/491.long

Mayer, M. L., I. Pot, M. Chang, H. Xu, V. Aneliunas *et al.*, 2004   Identification of protein complexes required for efficient sister chromatid cohesion. Mol. Biol. Cell 15: 1736–1745. https://doi.org/10.1091/mbc.e03-08-0619

McVey, M., V. Y. Khodaverdian, D. Meyer, P. G. Cerqueira, and W.-D. Heyer, 2016   Eukaryotic DNA polymerases in homologous recombination. Annu. Rev. Genet. 50: 393–421. https://doi.org/10.1146/annurev-genet-120215-035243

Mekhail, K., J. Seebacher, S. P. Gygi, and D. Moazed, 2008   Role for perinuclear chromosome tethering in maintenance of genome stability. Nature 456: 667–670. https://doi.org/10.1038/nature07460

Milgrom, E., H. Diab, F. Middleton, and P. M. Kane, 2007   Loss of vacuolar proton-translocating ATPase activity in yeast results in chronic oxidative stress. J. Biol. Chem. 282: 7125–7136. https://doi.org/10.1074/jbc.M608293200

Mohanty, B. K., N. K. Bairwa, and D. Bastia, 2006   The Tof1p-Csm3p protein complex counteracts the Rrm3p helicase to control replication termination of *Saccharomyces cerevisiae*. Proc. Natl. Acad. Sci. USA 103: 897–902. https://doi.org/10.1073/pnas.0506540103

Morano, K. A., C. M. Grant, and W. S. Moye-Rowley, 2012   The response to heat shock and oxidative stress in *Saccharomyces cerevisiae*. Genetics 190: 1157–1195. https://doi.org/10.1534/genetics.111.128033

Myung, K., A. Datta, C. Chen, and R. D. Kolodner, 2001   *SGS1*, the *Saccharomyces cerevisiae* homologue of BLM and WRN, suppresses genome instability and homeologous recombination. Nat. Genet. 27: 113–116. https://doi.org/10.1038/83673

Nicholson, A., M. Hendrix, S. Jinks-Robertson, and G. F. Crouse, 2000   Regulation of mitotic homeologous recombination in yeast: functions of mismatch repair and nucleotide excision repair genes. Genetics 154: 133–146. https://www.genetics.org/content/154/1/133.long

Noguchi, E., C. Noguchi, L.-L. Du, and P. Russell, 2003   Swi1 prevents replication fork collapse and controls checkpoint kinase Cds1. Mol. Cell. Biol. 23: 7861–7874. https://doi.org/10.1128/MCB.23.21.7861-7874.2003

Noguchi, E., C. Noguchi, W. H. McDonald, J. R. Yates, and P. Russell, 2004   Swi1 and Swi3 are components of a Replication Fork Protection Complex in fission yeast. Mol. Cell. Biol. 24: 8342–8355. https://doi.org/10.1128/MCB.24.19.8342-8355.2004

Novarina, D., G. E. Janssens, K. Bokern, T. Schut, N. C. van Oerle *et al.*, 2020   A genome-wide screen identifies genes that suppress the accumulation of spontaneous mutations in young and aged yeast cells. Aging Cell 19: e13084. https://doi.org/10.1111/acel.13084

O'Connell, K., S. Jinks-Robertson, and T. D. Petes, 2015   Elevated Genome-wide instability in yeast mutants lacking RNase H activity. Genetics 201: 963–975. https://doi.org/10.1534/genetics.115.182725

Owiti, N., C. Lopez, S. Singh, A. Stephenson, and N. Kim, 2017   Def1 and Dst1 play distinct roles in repair of AP lesions in highly transcribed

genomic regions. DNA Repair (Amst.) 55: 31–39. https://doi.org/10.1016/j.dnarep.2017.05.003

Pan, X., P. Ye, D. S. Yuan, X. Wang, J. S. Bader *et al.*, 2006 A DNA integrity network in the yeast *Saccharomyces cerevisiae*. Cell 124: 1069–1081. https://doi.org/10.1016/j.cell.2005.12.036

Poon, B. P. K., and K. Mekhail, 2011 Cohesin and related coiled-coil domain-containing complexes physically and functionally connect the dots across the genome. Cell Cycle 10: 2669–2682. https://doi.org/10.4161/cc.10.16.17113

Popoff, S. C., A. I. Spira, A. W. Johnson, and B. Demple, 1990 Yeast structural gene (*APN1*) for the major apurinic endonuclease: homology to *Escherichia coli* endonuclease IV. Proc. Natl. Acad. Sci. USA 87: 4193–4197. https://doi.org/10.1073/pnas.87.11.4193

Potenski, C. J., H. Niu, P. Sung, and H. L. Klein, 2014 Avoidance of ribonucleotide-induced mutations by RNase H2 and Srs2-Exo1 mechanisms. Nature 511: 251–254. https://doi.org/10.1038/nature13292

Prado, F., and A. Aguilera, 2005 Partial depletion of histone H4 increases homologous recombination-mediated genetic instability. Mol. Cell. Biol. 25: 1526–1536. https://doi.org/10.1128/MCB.25.4.1526-1536.2005

Prakash, S., and L. Prakash, 2000 Nucleotide excision repair in yeast. Mutat. Res. 451: 13–24. https://doi.org/10.1016/S0027-5107(00)00037-3

Saugar, I., J. L. Parker, S. Zhao, and H. D. Ulrich, 2012 The genome maintenance factor Mgs1 is targeted to sites of replication stress by ubiquitylated PCNA. Nucleic Acids Res. 40: 245–257. https://doi.org/10.1093/nar/gkr738

Schalbetter, S. A., S. Mansoubi, A. L. Chambers, J. A. Downs, and J. Baxter, 2015 Fork rotation and DNA precatenation are restricted during DNA replication to prevent chromosomal instability. Proc. Natl. Acad. Sci. USA 112: E4565–E4570. https://doi.org/10.1073/pnas.1505356112

Schmidt, K. H., and R. D. Kolodner, 2004 Requirement of Rrm3 helicase for repair of spontaneous DNA lesions in cells lacking Srs2 or Sgs1 helicase. Mol. Cell. Biol. 24: 3213–3226. https://doi.org/10.1128/MCB.24.8.3213-3226.2004

Schneider, C. A., W. S. Rasband, and K. W. Eliceiri, 2012 NIH Image to ImageJ: 25 years of image analysis. Nat. Methods 9: 671–675. https://doi.org/10.1038/nmeth.2089

Sherman, F., 2002 Getting started with yeast. Methods Enzymol. 350: 3–41 https://doi.org/10.1016/S0076-6879(02)50954-X

Smith, J., and R. Rothstein, 1999 An allele of *RFA1* suppresses *RAD52*-dependent double-strand break repair in *Saccharomyces cerevisiae*. Genetics 151: 447–458. https://www.genetics.org/content/151/2/447.long

Sommariva, E., T. K. Pellny, N. Karahan, S. Kumar, J. A. Huberman *et al.*, 2005 *Schizosaccharomyces pombe* Swi1, Swi3, and Hsk1 are components of a novel S-phase response pathway to alkylation damage. Mol. Cell. Biol. 25: 2770–2784. https://doi.org/10.1128/MCB.25.7.2770-2784.2005

Spell, R. M., and S. Jinks-Robertson, 2004 Examination of the roles of Sgs1 and Srs2 helicases in the enforcement of recombination fidelity in *Saccharomyces cerevisiae*. Genetics 168: 1855–1865. https://doi.org/10.1534/genetics.104.032771

Spies, M., and R. Fishel, 2015 Mismatch repair during homologous and homeologous recombination. Cold Spring Harb. Perspect. Biol. 7: a022657. https://doi.org/10.1101/cshperspect.a022657

Stirling, P. C., M. S. Bloom, T. Solanki-Patil, S. Smith, P. Sipahimalani *et al.*, 2011 The complete spectrum of yeast chromosome instability genes identifies candidate CIN cancer genes and functional roles for ASTRA complex components. PLoS Genet. 7: e1002057. https://doi.org/10.1371/journal.pgen.1002057

Styles, E. B., K. J. Founk, L. A. Zamparo, T. L. Sing, D. Altintas *et al.*, 2016 Exploring quantitative yeast phenomics with single-cell analysis of DNA damage foci. Cell Syst. 3: 264–277.e10. https://doi.org/10.1016/j.cels.2016.08.008

Sugawara, N., T. Goldfarb, B. Studamire, E. Alani, and J. E. Haber, 2004 Heteroduplex rejection during single-strand annealing requires Sgs1 helicase and mismatch repair proteins Msh2 and Msh6 but not Pms1. Proc. Natl. Acad. Sci. USA 101: 9315–9320. https://doi.org/10.1073/pnas.0305749101

Supek, F., M. Bošnjak, N. Škunca, and T. Šmuc, 2011 REVIGO summarizes and visualizes long lists of Gene Ontology terms. PLoS One 6: e21800. https://doi.org/10.1371/journal.pone.0021800

Swanson, R. L., N. J. Morey, P. W. Doetsch, and S. Jinks-Robertson, 1999 Overlapping specificities of base excision repair, nucleotide excision repair, recombination, and translesion synthesis pathways for DNA base damage in *Saccharomyces cerevisiae*. Mol. Cell. Biol. 19: 2929–2935. https://doi.org/10.1128/MCB.19.4.2929

Symington, L. S., R. Rothstein, and M. Lisby, 2014 Mechanisms and regulation of mitotic recombination in *Saccharomyces cerevisiae*. Genetics 198: 795–835. https://doi.org/10.1534/genetics.114.166140

Thorpe, G. W., C. S. Fong, N. Alic, V. J. Higgins, and I. W. Dawes, 2004 Cells have distinct mechanisms to maintain protection against different reactive oxygen species: Oxidative-stress-response genes. Proc. Natl. Acad. Sci. USA 101: 6564–6569. https://doi.org/10.1073/pnas.0305888101

Torres, J. Z., S. L. Schnakenberg, and V. A. Zakian, 2004 *Saccharomyces cerevisiae* Rrm3p DNA helicase promotes genome integrity by preventing replication fork stalling: viability of *rrm3* cells requires the intra-S-phase checkpoint and fork restart activities. Mol. Cell. Biol. 24: 3198–3212. https://doi.org/10.1128/MCB.24.8.3198-3212.2004

Treco, D. A., and V. Lundblad, 2001 Preparation of yeast media. *Curr. Protoc. Mol. Biol.* Chapter 13: Unit13.1. https://doi.org/10.1002/0471142727.mb1301s23

Tsurimoto, T., A. Shinozaki, M. Yano, M. Seki, and T. Enomoto, 2005 Human Werner helicase interacting protein 1 (WRNIP1) functions as a novel modulator for DNA polymerase delta. Genes Cells 10: 13–22. https://doi.org/10.1111/j.1365-2443.2004.00812.x

Ulrich, H. D., 2005 The *RAD6* pathway: Control of DNA damage bypass and mutagenesis by ubiquitin and SUMO. ChemBioChem 6: 1735–1743. https://doi.org/10.1002/cbic.200500139

Umemoto, N., Y. Ohya, and Y. Anraku, 1991 *VMA11*, a novel gene that encodes a putative proteolipid, is indispensable for expression of yeast vacuolar membrane H$^+$-ATPase activity. J. Biol. Chem. 266: 24526–24532. https://www.jbc.org/content/266/36/24526.long

Urtishak, K. A., K. D. Smith, R. A. Chanoux, R. A. Greenberg, F. B. Johnson *et al.*, 2009 Timeless maintains genomic stability and suppresses sister chromatid exchange during unperturbed DNA replication. J. Biol. Chem. 284: 8777–8785. https://doi.org/10.1074/jbc.M806103200

Usaj, M., Y. Tan, W. Wang, B. VanderSluis, A. Zou *et al.*, 2017 TheCellMap.org: a web-accessible database for visualizing and mining the global yeast genetic interaction network. G3 (Bethesda) 7: 1539–1549. https://doi.org/10.1534/g3.117.040220

Vance, J. R., and T. E. Wilson, 2001 Repair of DNA strand breaks by the overlapping functions of lesion-specific and non-lesion-specific DNA 3′ phosphatases. Mol. Cell. Biol. 21: 7191–7198. https://doi.org/10.1128/MCB.21.21.7191-7198.2001

Veatch, J. R., M. A. McMurray, Z. W. Nelson, and D. E. Gottschling, 2009 Mitochondrial dysfunction leads to nuclear genome instability via an iron-sulphur cluster defect. Cell 137: 1247–1258. https://doi.org/10.1016/j.cell.2009.04.014

Warde-Farley, D., S. L. Donaldson, O. Comes, K. Zuberi, R. Badrawi *et al.*, 2010 The GeneMANIA prediction server: biological network integration for gene prioritization and predicting gene function. Nucleic Acids Res. 38: W214–W220. https://doi.org/10.1093/nar/gkq537

Wong, C. M., K. L. Siu, and D. Y. Jin, 2004 Peroxiredoxin-null yeast cells are hypersensitive to oxidative stress and are genomically unstable. J. Biol. Chem. 279: 23207–23213. https://doi.org/10.1074/jbc.M402095200

Wu, L., C. Z. Bachrati, J. Ou, C. Xu, J. Yin *et al.*, 2006 BLAP75/RMI1 promotes the BLM-dependent dissolution of homologous recombination intermediates. Proc. Natl. Acad. Sci. USA 103: 4068–4073. https://doi.org/10.1073/pnas.0508295103

Xia, L., L. Jaafar, A. Cashikar, and H. Flores-Rozas, 2007 Identification of genes required for protection from doxorubicin by a genome-wide screen in *Saccharomyces cerevisiae*. Cancer Res. 67: 11411–11418. https://doi.org/10.1158/0008-5472.CAN-07-2399

Xiao, W., and L. Samson, 1993 *In vivo* evidence for endogenous DNA alkylation damage as a source of spontaneous mutation in eukaryotic cells.

Proc. Natl. Acad. Sci. USA 90: 2117–2121. https://doi.org/10.1073/pnas.90.6.2117

Xu, H., C. Boone, and H. L. Klein, 2004   Mrc1 is required for sister chromatid cohesion to aid in recombination repair of spontaneous damage. Mol. Cell. Biol. 24: 7082–7090. https://doi.org/10.1128/MCB.24.16.7082-7090.2004

Yang, J., C. Z. Bachrati, J. Ou, I. D. Hickson, and G. W. Brown, 2010   Human topoisomerase IIIα is a single-stranded DNA decatenase that is stimulated by BLM and RMI1. J. Biol. Chem. 285: 21426–21436. https://doi.org/10.1074/jbc.M110.123216

Yi, D. G., M. J. Kim, J. E. Choi, J. Lee, J. Jung et al., 2016   Yap1 and Skn7 genetically interact with Rad51 in response to oxidative stress and DNA double-strand break in Saccharomyces cerevisiae. Free Radic. Biol. Med. 101: 424–433. https://doi.org/10.1016/j.freeradbiomed.2016.11.005

Zhang, C., 2014   Essential functions of iron-requiring proteins in DNA replication, repair and cell cycle control. Protein Cell 5: 750–760. https://doi.org/10.1007/s13238-014-0083-7

Communicating editor: N. Rhind